



THE UNIVERSITY *of* EDINBURGH

Edinburgh Research Explorer

Sub-millisecond ligand probing of cell receptors with multiple solution exchange

Citation for published version:

Sylantsev, S & Rusakov, DA 2013, 'Sub-millisecond ligand probing of cell receptors with multiple solution exchange' Nature Protocols, vol 8, no. 7, pp. 1299-1306., 10.1038/nprot.2013.075

Digital Object Identifier (DOI):

[10.1038/nprot.2013.075](https://doi.org/10.1038/nprot.2013.075)

Link:

[Link to publication record in Edinburgh Research Explorer](#)

Document Version:

Author final version (often known as postprint)

Published In:

Nature Protocols

Publisher Rights Statement:

Published in final edited form as:

Nat Protoc. 2013 July; 8(7): 1299–1306.

Published online 2013 June 6. doi: 10.1038/nprot.2013.07

General rights

Copyright for the publications made accessible via the Edinburgh Research Explorer is retained by the author(s) and / or other copyright owners and it is a condition of accessing these publications that users recognise and abide by the legal requirements associated with these rights.

Take down policy

The University of Edinburgh has made every reasonable effort to ensure that Edinburgh Research Explorer content complies with UK legislation. If you believe that the public display of this file breaches copyright please contact openaccess@ed.ac.uk providing details, and we will remove access to the work immediately and investigate your claim.



Published in final edited form as:

Nat Protoc. 2013 July ; 8(7): 1299–1306. doi:10.1038/nprot.2013.075.

Sub-millisecond ligand probing of cell receptors with multiple solution exchange

Sergiy Sylantsev and Dmitri A Rusakov

UCL Institute of Neurology, University College London, London, UK

Abstract

The accurate knowledge of receptor kinetics is crucial to our understanding of cell signal transduction in general and neural function in particular. The classical technique of probing membrane receptors on a millisecond scale involves placing a recording micropipette with a membrane patch in front of a double-barrel (θ -glass) application pipette mounted on a piezo actuator. Driven by electric pulses, the actuator can rapidly shift the θ -glass pipette tip, thus exposing the target receptors to alternating ligand solutions. However, membrane patches survive for only a few minutes, thus normally restricting such experiments to a single-application protocol. In order to overcome this deficiency, we have introduced pressurized supply microcircuits in the θ -glass channels, thus enabling repeated replacement of application solutions within 10–15 s. This protocol, which has been validated in our recent studies and takes 20–60 min to implement, allows the characterization of ligand-receptor interactions with high sensitivity, thereby also enabling a powerful paired-sample statistical design.

INTRODUCTION

Background

Activation of cell membrane receptors by extracellular ligands is a fundamental mechanism of signal transduction in live organisms. More specifically, accurate knowledge of synaptic receptor kinetics has been crucial to our understanding of how the elementary informative signals are processed and stored by the neural circuit machinery of the brain. Once a neurotransmitter has been released into the synaptic cleft, its local concentration initially peaks and then drops substantially within 200–300 μ s. Because this time span is often much shorter than the characteristic open time of synaptic receptor channels, their activation typically occurs in conditions of substantial nonequilibrium^{1–3}. Consequently, the classical kinetic-equilibrium measures, such as the dissociation constant K_d , are unlikely to explain the synaptic receptor activation kinetics from the local neurotransmitter concentration in the extracellular space. Indeed, experimental evidence commonly points to a complex relationship between the time course of individual synaptic responses and the waveform of the local neurotransmitter transient in central synapses. Therefore, probing receptor activation on the sub-millisecond time scale should be an important empirical strategy for obtaining receptor kinetics and the ligand pharmacological profile under conditions that closely reproduce physiological synaptic events.

© 2013 Nature America, Inc. All rights reserved.

Correspondence should be addressed to D.A.R. (d.rusakov@ucl.ac.uk) or S.S. (s.sylantsev@ucl.ac.uk).

AUTHOR CONTRIBUTIONS S.S. carried out the experimental studies; D.A.R. and S.S. designed the protocol, analyzed the data and wrote the paper.

COMPETING FINANCIAL INTERESTS The authors declare no competing financial interests.

Note: Supplementary information is available in the online version of the paper.

Historical and existing techniques

Three decades ago, several techniques had been developed to provide rapid ligand application to an excised cell soma or a cell membrane patch. A side-pore perfusion system⁴ and a single-filament application probe driven by a piezo element⁵ were described in the 1980s. Subsequently, various experimental systems were implemented that enable application of multiple solutions to the recorded patch, such as a piezo-driven multicapillary application pipette⁶, U-tube perfusion⁷ or a plumbing flow-exchange method⁸. Repeated application of different solutions within the lifetime of a membrane patch (1–5 min) should be a crucial advantage in many experimental designs: successive pharmacological manipulations on the same receptor pool (e.g., to document activation, washout, blockade and so on) are key to the reliable receptor characterization and, in turn, to the development of pharmacological tools. However, the aforementioned techniques operate with ligand exposure times exceeding 10–100 ms, which is substantially slower than extracellular neurotransmitter transients generated locally by small central synapses. To achieve sub-millisecond application times in excised patches (outside organized tissue), a system was therefore developed, which relied on a double-barrel (θ -glass) piezo-driven micropipette^{9–13}, with an estimated time response limit of $\sim 20 \mu\text{s}$ (ref. 14). Inside organized tissue, fast application times could be achieved, albeit with little control over precise ligand concentrations, by using common iontophoretic electrode ejection with a two-pipette (source-sink) system¹⁵, or, more recently, by using rapid photolytic neurotransmitter release (uncaging)¹⁶. It would be important, however, to combine sub-millisecond ligand application with the capacity of multiple solution exchange. The elegant method of a hydraulic flow switch¹⁷ can in principle provide this combination, but it has some crucial limitations, especially in experiments involving membrane patches excised from cells *in situ*. First, multiple application capillaries are mounted on the objective providing a prefixed focal plane site where the application takes place¹⁷. This must restrict, if not entirely prevent, microscopic exploration of tissue and selection of target cells *in situ*. Second, the method uses aqueous streams flowing from different directions: a rapid switch between such streams can introduce a mechanical concomitant and shorten preparation lifetime, especially with relatively bulky nucleated patches (somatic envelopes).

Experimental design

Our aim was to develop a simple technique in which ligand solutions applied with the piezo-driven θ -glass pipette could be fully replaced during the lifetime of individual cell membrane patches (1–5 min). To achieve this, we introduced several modifications described below and termed thereafter a rapid application and solution exchange (RASE) protocol. The approach has been validated in several of our research publications, as illustrated below, involving not only the standard outside-out membrane patches but also larger nucleated patches (nucleus-containing somatic envelopes) that preserve the somatic milieu in tested cells.

It has been noted previously that, with the θ -glass configuration, the flow velocity has to be below $100\text{--}150 \mu\text{m ms}^{-1}$ to avoid damaging the patch and that the optimal pipette tip diameter must be $\sim 200 \mu\text{m}$. Although rapid application relies on the mechanics of the piezo-driven θ -glass pipette tip movements, the replacement of applied solutions inside the two barrels depends on rapid solution supply from the back end. The supply could be arranged by having, inside the barrels, one or more flexible microfilaments connected to a pressurized microtube circuit. However, this arrangement typically yields a relatively slow rate of solution exchange, most likely due to a relatively large dead volume (buffering capacity) inside θ -glass channels, leading to a substantial initial dilution and local vortex formation. Speeding up the exchange by increasing supply pressure is counteracted by the considerable viscous resistance in the thin filaments and can also damage the patch. We therefore set out

to increase the solution exchange rate by reducing the dead solution volume inside the θ -glass pipette.

Multiple-circuit application pipette—We set out to have three or four supply circuit microfilaments in each θ -glass channel while maximally reducing the solution exchange volume (Fig. 1a). To achieve this, we developed the procedure as follows. First, we inserted three microfilaments in one θ -glass barrel roughly realigning their ends near the pipette tip (Fig. 1b). Second, we connected a fourth microfilament to a syringe filled with a rapidly setting, water-resistant glue and inserted it into the same channel (Fig. 1b, image 3). Pressure was applied to inject the glue into the glass-channel filling before it reached the three filament ends (Fig. 1b). The procedure was repeated for the other θ -glass barrel (Fig. 1b). Once the glue was set, the pipette was ready for use (Fig. 1c) and could be mounted on the piezo-actuator attached to a standard microelectrode holder (Fig. 1d) and electrically connected to a standard constant-voltage stimulus isolator. The pipette mount was made out of a three-way plastic tubing adaptor, with one branch cut off to provide a channel for the tightening screw (Fig. 1d, inset).

Pressurized circuit for multiple solution exchange—In the typical configuration, the solution supply circuit contained three plastic solution containers (from a blood dialysis kit) for each pipette barrel. Each of these containers was connected to a pressure supply line and was equipped with three-way taps and a replaceable stopcock (Fig. 2a,b). Two separate pressure supplies (standard micropumps) were normally required to adjust and equalize pressure and therefore the ejected stream speed, between the two barrels (which normally show slightly different hydraulic resistance). Application solutions could be added to each container independently through a three-way tap with a stopcock removed to siphon the air inside (Fig. 2a,b). Because switching the solution supply is likely to generate pulses of excessive pressure, pressure-buffering microfilters were inserted between the solution container and each loading capillary (Fig. 2c).

Optimizing pipette position and speed—To ensure the fastest possible application time, the membrane patch needs to be as close as possible to the piezo-driven application pipette. At the same time, it is important to avoid flow distortions and fluctuations in the streams when they exit the θ -glass and meet at the end of the glass dividing wall (septum) (Fig. 3a). We therefore routinely placed a recording pipette at a distance of 20–30 μm from the tip and further adjusted its position using the water test (Fig. 3b and Supplementary Video 1). Positioning the patch at some distance from the θ -glass pipette has another important advantage: because of the brief delay between the θ -glass movement onset and the time the mechanical wave reaches the recorded patch, there is a clear time lag between the electrical artifact from the piezo-actuator switch and the actual membrane receptor response (Fig. 3b). This can be helpful in separating the pulse from the concomitant artifact.

A small piece of silicone inserted into the θ -glass pipette holder under the tightening screw (Fig. 1d) and the use of shorter pipettes (where possible) can also help in reducing flow fluctuations (Fig. 3a). The speed at which the application solution switches depends on the rate of piezo-actuator bending and the length of the application θ -glass pipette attached to it. This speed could be boosted, at least in theory, either by strengthening the electrical pulse applied to the piezo actuator or by using longer pipettes (and thus speeding up their tip movement). In practice, however, increasing the pipette length leads to concomitant problems such as increased tip vibration and reduced pipette maneuverability. In addition, longer θ -glass pipettes require longer loading microfilaments, thus increasing viscous resistance to solution flow.

Maintaining the correct temperature of the applied solution is important for reliable characterization of tested receptors. Therefore, in order to ensure temperature equilibration, the tip of the θ -glass pipette should be submerged into perfusion solution for at least 4–5 mm before starting the recording session. Temperature control in the application streams can be performed by placing a microthermocouple (e.g., Cole-Palmer Type-K, straight-shaft microprobe, tip diameter $\sim 100\ \mu\text{m}$, precision $\pm 1\ ^\circ\text{C}$) at the position of the patch recording electrode tip.

Experimental validation

The present RASE protocol has been validated in our recent studies, in which cell patches were excised from acute brain slices, focusing on hippocampal CA1 pyramidal cells^{18–20}, granule cells²¹, cerebellar granule cells (CGCs)^{18,20} and cultured CGCs¹⁸. In one example²¹, we tested the solution exchange system on its own, by recording single-channel currents of γ -aminobutyric acid A (GABA)_A receptors to establish receptor sensitivity to GABA and to the common antagonists (Fig. 4a,b). An example from another recent study¹⁸ reveals the sensitivity of 2-amino-3-(3-hydroxy-5-methyl-isoxazol-4-yl)propanoic acid (AMPA) receptors to the competitive antagonist γ -D-glutamylglycine when 1 mM–1 ms pulses of glutamate are applied in a single patch from CA1 pyramidal cells (Fig. 4c).

In a related work, the RASE enabled us to test a hypotheses according to which perisynaptic group I metabotropic glutamate receptors (mGluRs) could rapidly, on a sub-millisecond scale, boost local synaptic *N*-methyl-D-aspartate (NMDA) receptor (NMDAR) currents in CGCs²⁰. Our experimental objectives thus were to enable receptor probing on a sub-millisecond scale, to isolate receptor responses from any network influences and to preserve, as much as possible, the postsynaptic protein machinery. We therefore carried out RASE experiments in nucleated patches of CGCs (Fig. 5a): we applied a 1-ms pulse of 1 mM glutamate (plus 1 mM glycine) to compare evoked NMDAR currents between control conditions and after adding group I mGluR antagonists LY367385 (LY, 100 μM) and 2-methyl-6-(phenylethynyl)pyridine (MPEP, 200 nM) to both θ -glass barrels (solution exchange took ~ 10 s). The NMDAR specificity in the patch was further tested using a third solution exchange, which added the NMDAR antagonist APV (50 μM). We found that NMDAR responses to the same pulse, in the same membrane patch, were inhibited by group-I metabotropic glutamate receptor (mGluR) antagonists (Fig. 5b). This result indicated that a 1-ms exposure of mGluRs to glutamate was sufficient to boost NMDAR currents activated by the same glutamate pulse. This effect was not due to contaminant actions of LY + MPEP or the constituent activity of mGluRs because the same experiment with NMDA applied instead of glutamate showed no mGluR blockade on NMDARs (Fig. 5c; see further data and detailed explanations in the original research report²⁰).

Advantages and limitations

The principal advantage of RASE is that it allows the application of several different ligands in a single rapid solution application experiment probing the same receptor pool. Because the effect of interest could be relatively modest and/or smaller than the variation between cells or patches recorded in separate experiments, the RASE protocol greatly enhances the experimental design through the use of paired-sample statistics. Combined with recordings from nucleated patches, RASE also allows experimental separation of the effects pertinent to the intracellular machinery of receptor action on the sub-millisecond scale. In a more general context, RASE could be applied to the fields of research outside patch-clamp electrophysiology, such as protein-ligand interactions in biophysical or biochemical assays, non-neuronal cell physiology or materials science.

There are several potential limitations of RASE. First, in the case of nerve cells, this and similar rapid application techniques are designed to probe predominantly extrasynaptic receptors exposed to the application medium. Indeed, we have recently shown that the externally applied concentration pulse is slowed down while reaching target receptors inside the synaptic cleft²⁰. Second, because of the variable characteristics of θ -glass pipettes (profile of the tip, size of the dead space inside, widths of the two barrels and so on) such pipettes should be individually calibrated to find a suitable pressure in each channel, the amplitude and duration of the electric switching pulse and the recording pipette position. Third, in nucleated patches, the turbulence at the patch side opposite to the application side could have a variable (albeit relatively small) effect on the kinetics of recorded receptor responses. In our experience, however, this concomitant effect could be satisfactorily averaged out with an increased number of recorded individual traces.

Below we detail the RASE protocol setup for recording of receptor responses to sub-millisecond application of receptor ligands. Here we routinely refer the reader to the textbook details of brain slice preparation, whole-cell patch-clamp methods²²⁻²⁴, the outside-out patch technique²⁵ and nucleated patch configuration²⁶ patches. Therefore, standard electrophysiological procedures and equipment will not be discussed unless they are specifically important to the procedure or to its troubleshooting. Substantial hands-on experience in standard electrophysiological patch-clamp techniques is expected for a successful implementation of the present protocol.

MATERIALS

REAGENTS

- *In vitro* preparation. The present protocol can be used with a variety of *in vitro* preparations suitable for whole-cell recordings, from acute brain slices to cell cultures
- Standard salts and reagents for preparing electrophysiological solutions: CaCl₂, glucose, HEPES, KCH₃O₃S, KCl, KOH, MgCl₂, MgSO₄, Na₂-ATP, NaCl, Na-GTP, NaHCO₃, NaH₂PO₄, Na₂-Phosphocreatine (all from Sigma-Aldrich)
- Deionized water, at least 15 M Ω cm at 25 °C; note that water quality is important for recording pipette solutions
- Receptor ligands and drugs. These should be obtained from reliable sources in accordance with the experimental design

EQUIPMENT

- A standard setup for electrophysiology, including a submerged type recording chamber (for acute slices or cell cultures) equipped with $\times 20$ – 60 IR differential interference contrast (DIC) visualization, a patch-clamp amplifier capable of current and voltage clamp (e.g., MultiClamp 700B), multichannel digitizer (e.g., Digidata 1440A), constant-voltage stimulus isolator (e.g., DS2, Digitimer) and double-channel pneumatic drug ejector (e.g., PDES-02DX, NPI Electronics) ▲ **CRITICAL** Optimized IR DIC optics with the $\times 20$ – 60 objective (with further $\times 2$ – 4 magnification) is important for visualizing neurons and reliable control of the patch pulling process up to 100–150- μ m deep inside the brain slice, where the cell physiology is least perturbed.
- Patch electrodes pulled from borosilicate glass (e.g., GF150F-3, Warner Instruments). Pipettes of 5–6-M Ω resistance appear to be well suited for experiments on outside-out patches, whereas for nucleated patches the optimal

pipette resistance is somewhat lower (4–5 M Ω); fire polishing of pipette ends substantially increases the lifespan of a patch

- Borosilicate θ -capillary glass (e.g., TGC150-7.5, Harvard Apparatus)
- Solution loading microfilaments (e.g., MF34G, World Precision Instruments)
- Bender piezoelectric actuators with stranded wires (e.g., PL127.11, Physik Instrumente)
- Rapidly hardening glue (e.g., cyanoacrylate glue)

PROCEDURE

Assembling the rapid application pipette ● TIMING 1–2 h (excluding glue setting)

- 1| Pull the solution application pipette with a \sim 200- μ m tip from θ -glass capillary using a standard pipette puller and fix it under a low-magnification binocular microscope, e.g., using blue tack (Fig. 1b).
- 2| Insert the supply microfilaments into one barrel and fix them in a position, e.g., with a piece of blue tack placed near the pipette blunt end (Fig. 1b).
- 3| Insert another freely moving microfilament connected to a syringe filled with glue (Fig. 1b).
- 4| Gently eject the glue by applying pressure with the syringe; stop ejection when the glue approaches the ends of the supply microfilaments (Fig. 1b).

▲ **CRITICAL STEP** The stop point should be at least 1.5–2-mm away from the ends of the supply microfilaments.

This is to prevent drawing of the glue inside the filaments by capillary forces.

? TROUBLESHOOTING

- 5| Slowly remove the filament connected to the syringe with glue; if you experience difficulty, leave it inside the barrel and later cut at a pipette end.
- 6| Repeat Steps 2–5 for the other barrel of the θ -glass pipette (Fig. 1b).
- 7| Leave the pipette for several hours (overnight) to let the glue set inside the barrels (Fig. 1c).
- 8| Glue the piezo actuator to the holding rod and glue a pipette holder of an appropriate size to the side of the actuator (Fig. 1d).

Assembling the pressurized solution supply system ● TIMING 0.5–1 h

- 9| Prepare containers for the application solutions (e.g., use syringes for gravity-driven perfusion systems or plastic containers from a standard blood dialysis kit for closed pump-operated systems), in accordance with the number of supply microfilaments in the θ -glass pipette (Fig. 2a,b). Equip each such container with a tap connector and an outlet with an air-tight cap, e.g., by using thick syringe needles glued or melted into the container body plastic (Fig. 2a,b). Place containers in a suitable position near the recording setup.
- 10| Connect two groups of containers (each to supply one of the θ -glass pipette channels) to the gas supply lines using thin tubing (e.g., Tygon 1/32-inch tubing).

- 11| In accordance with the available micropump hardware, connect the pneumatic ejector inlets to the source of pressurized inert gas (nitrogen), and connect the outlets to the lines supplying pressure for the two groups of containers (Fig. 2a,b).
- 12| Clamp the piezo-actuator rod in microelectrode holder; connect wires of the piezo actuator to the output sockets of a constant-voltage stimulus isolator. Insert the solution application pipette into the pipette holder; connect loading microfilaments of the two θ -glass barrels to the corresponding groups of containers using thin tubing (Fig. 2c).
 - ▲ **CRITICAL STEP** Insert a microfilter connector between the container and the loading capillary to buffer excessive pressure jumps in the system (Fig. 1d).

? TROUBLESHOOTING

System calibration and experimental setting ● TIMING 2–4 h

- 13| To test solution exchange times, fill containers of the solution supply system with artificial cerebrospinal fluid (ACSF) and with distilled water using syringe inlets (Fig. 2a,b) such that each θ -glass pipette barrel can be supplied with the alternating liquids. Apply pressure to the system to fully fill the supply microfilaments and the pipette dead volume. Because of the different optical characteristics of distilled water and ACSF, the corresponding ejection streams show a visible interface and the outer boundaries; use this indicator to adjust the recording pipette position (Supplementary Video 1). Alternatively, use different water-soluble inert inks or dyes added to each solution.
- 14| Submerge the solution application pipette into the recording chamber and focus the microscope on its tip.
- 15| Place the patch-clamp recording electrode filled with a standard intracellular solution under the microscope close to the θ -glass pipette tip; open solution supply lines so that different liquids come from the barrels. Trigger the stimulus isolator to rapidly shift the streams near the tip of the open patch pipette.
- 16| Adjust the settings of the stimulus isolator (applied voltage, voltage step length), the *XYZ* patch pipette position and ejection pressure at both θ -glass channels in order to maximize the solution switch speed reflected in the recorded current pulse (Fig. 3). Locate the optimum *XYZ* recording pipette tip position by placing it near the visible stream interface.
- 17| Test the system for pulse lengths and solution replacement periods (inside θ -glass barrels) in accordance with the required protocol. If the ejection stream fails because of the unlikely event of one or more clogged channels, use other channels or replace the application pipette.
- 18| Once the system has been calibrated, manipulate the recording patch pipette into the slice (or culture) preparation. This should be done first in order to hold the target cell in whole-cell mode and second to pull an outside-out or a nucleated patch, in accordance with well-established electrophysiological procedures (Supplementary Videos 2 and 3).

Protocol implementation in a patch experiment ● TIMING 20–60 min

- 19| Place the recording pipette tip containing the patch into the optimal *XYZ* position established and noted during the calibration procedure (Step 16). Start your experiment as per your protocol.

System maintenance ● TIMING 20–30 min

- 20| After an experiment, thoroughly rinse the whole setup (pressurized solution supply system, θ -glass pipette) with ~20% (vol/vol) ethanol and distilled water, and then blow it dry with an inert gas at high pressure.

▲ **CRITICAL STEP** The θ -glass pipette tip and, especially, loading microfilaments are extremely sensitive to blocking with dust and precipitated crystals. Therefore, it is absolutely necessary to treat all used solutions using 4–10- μ m filters and to perform extensive rinsing after each experiment.

? TROUBLESHOOTING**? TROUBLESHOOTING****Assembling the rapid solution application set (Step 4)**

The most crucial step in this preparation is the filling of θ -glass pipette with glue: capillary forces tend to draw the glue into the loading microfilaments and also toward θ -glass pipette tip. To overcome this, a drop of water can be placed at the sharp end of the pipette: on being pulled into the pipette tip by capillary forces, it forms a meniscus. Because the cyanoacrylate glue hardens rapidly upon contact with water, the water meniscus stops its progress toward the pipette end. If the minimal dead volume is not a crucial requirement (e.g., in experiments in which tested patches survive for longer than several minutes), filling with the glue can be stopped near the blunt end of the θ -glass pipette.

Optimizing the pressurized solution supply system (Step 12)

When the θ -glass pipette septum is not parallel to the piezo-bending actuator and/or the piezo-bending actuator is not perpendicular to the line of sight, it makes the system calibration much harder. In these conditions, it becomes difficult to optimize stimulus isolator settings and the recording pipette position (that provides a rapid enough switch between solutions). Therefore, one should pay attention when inserting the solution application pipette into the pipette holder and clamping the actuator rod in the micromanipulator holder.

System maintenance (Step 20)

Small amounts of solutions tend to accumulate toward the pipette tip because of the capillary force. It is sometimes virtually impossible to dry this remaining liquid even with gas blowing, and precipitated crystals can sometimes block the pipette tip, thus rendering the pipette unusable. To avoid this, after rinsing the pipette, dry it by touching its tip with a soft (lens) paper tissue, which absorbs the remaining solution.

● TIMING

Steps 1–12, assembling a rapid solution application set: 1 d; it is recommended that 5–7 sets should be manufactured and left overnight to let the superglue set

Steps 13–18, system calibration and experimental setting: 2–4 h, depending on the overall quality of prepared application sets

Step 19, protocol implementation in a patch experiment: 20–60 min, depending on the particular experimental design

Step 20, system maintenance: 20–30 min after the end of experimentation

ANTICIPATED RESULTS

The expected results will comprise traces of the receptor current recorded from individual outside-out or nucleated patches, normally divided into trial sweeps of 100–1,000 ms in length (Figs. 4 and 5). These data are routinely stored offline as binary or text files for subsequent analyses. The total number of trials per experiment is highly variable and depends on the patch stability and the particular experimental design. With a typical signal-to-noise ratio in this type of experimental recording, each experimental epoch (baseline-ligand-washout) should include at least three to five individual trials to ensure appropriate final averaging. Measured parameters of averaged traces should be analyzed using standard statistical methods, with an advantage of having real-time pharmacological manipulations in the same patch, thus enabling powerful paired-sample statistical tests. Normally, only one outside-out or nucleated patch is recorded in each individual acute brain slice with the RASE protocol, to avoid both contamination of the perfusion solution and accumulation of applied drugs in the tissue.

Supplementary Material

Refer to Web version on PubMed Central for supplementary material.

Acknowledgments

This work was supported by the Wellcome Trust, Medical Research Council (UK), the European Research Council (Advanced Grant), the European Commission COST Action BM1001 ECMNet, and the Biology and Biotechnology Research Council (UK).

References

1. Clements JD, Lester RA, Tong G, Jahr CE, Westbrook GL. The time course of glutamate in the synaptic cleft. *Science*. 1992; 258:1498–1501. [PubMed: 1359647]
2. Lisman JE, Raghavachari S, Tsien RW. The sequence of events that underlie quantal transmission at central glutamatergic synapses. *Nat. Rev. Neurosci.* 2007; 8:597–609. [PubMed: 17637801]
3. Zheng K, Scimemi A, Rusakov DA. Receptor actions of synaptically released glutamate: the role of transporters on the scale from nanometers to microns. *Biophys. J.* 2008; 95:4584–4596. [PubMed: 18689452]
4. Krishtal OA, Pidoplichko VI. A receptor for protons in the nerve cell membrane. *Neuroscience*. 1980; 5:2325–2327. [PubMed: 6970348]
5. Franke C, Hatt H, Dudel J. Liquid filament switch for ultra-fast exchanges of solutions at excised patches of synaptic membrane of crayfish muscle. *Neurosci. Lett.* 1987; 77:199–204. [PubMed: 2439957]
6. Raman IM, Trussell LO. The kinetics of the response to glutamate and kainate in neurons of the avian cochlear nucleus. *Neuron*. 1992; 9:173–186. [PubMed: 1352983]
7. Albuquerque EX, et al. Functional properties of the nicotinic and glutamatergic receptors. *J. Recept. Res.* 1991; 11:603–625. [PubMed: 1715922]
8. Brett RS, Dilger JP, Adams PR, Lancaster B. A method for the rapid exchange of solutions bathing excised membrane patches. *Biophys. J.* 1986; 50:987–992. [PubMed: 3790698]
9. Lester RAJ, Jahr CE. NMDA channel behavior depends on agonist affinity. *J. Neurosci.* 1992; 12:635–643. [PubMed: 1346806]
10. Tong G, Jahr CE. Multivesicular release from excitatory synapses of cultured hippocampal-neurons. *Neuron*. 1994; 12:51–59. [PubMed: 7507341]
11. Raman IM, Zhang S, Trussell LO. Pathway-specific variants of AMPA receptors and their contribution to neuronal signaling. *J. Neurosci.* 14:4998–5010. [PubMed: 7913958]

12. Colquhoun D, Jonas P, Sakmann B. Action of brief pulses of glutamate on AMPA/kainate receptors in patches from different neurones of rat hippocampal slices. *J. Physiol.* 1992; 458:261–287. [PubMed: 1338788]
13. Spruston N, Jonas P, Sakmann B. Dendritic glutamate-receptor channels in rat hippocampal CA3 and CA1 pyramidal neurons. *J. Physiol.* 1995; 482:325–352. [PubMed: 7536248]
14. Sachs F. Practical limits on the maximal speed of solution exchange for patch-clamp experiments. *Biophys. J.* 1999; 77:682–690. [PubMed: 10423417]
15. Veselovsky NS, Engert F, Lux HD. Fast local superfusion technique. *Pflugers Arch.* 1996; 432:351–354. [PubMed: 8662287]
16. Niu L, et al. Rapid chemical kinetic techniques for investigations of neurotransmitter receptors expressed in *Xenopus* oocytes. *Proc. Natl. Acad. Sci. USA.* 1996; 93:12964–12968. [PubMed: 8917527]
17. Maconochie DJ, Knight DE. A method for making solution changes in the sub-millisecond range at the tip of a patch pipette. *Pflugers Arch.* 1989; 414:589–596. [PubMed: 2780223]
18. Savtchenko LP, Sylant'ev S, Rusakov DA. Central synapses release a resource-efficient amount of glutamate. *Nat. Neurosci.* 2013; 16:10–12. [PubMed: 23242311]
19. Sylant'ev S, et al. Electric fields due to synaptic currents sharpen excitatory transmission. *Science.* 2008; 319:1845–1849. [PubMed: 18369150]
20. Sylant'ev S, Savtchenko LP, Ermolyuk Y, Michaluk P, Rusakov DA. Spike-driven glutamate electrodiffusion triggers synaptic potentiation via a Homer-dependent mGluR-NMDAR link. *Neuron.* 2013; 77:528–541. [PubMed: 23395378]
21. Wlodarczyk AI, et al. GABA-independent GABA_A receptor openings maintain tonic currents. *J. Neurosci.* 2013; 33:3905–3914. [PubMed: 23447601]
22. Marty, A.; Neher, E. Tight-seal whole-cell recording. In: Sakmann, B.; Neher, E., editors. *Single-Channel Recording*. Springer; 2009. p. 31-52.
23. Molleman, A. *Patch Clamping: An Introductory Guide To Patch-Clamp Electrophysiology*. J. Wiley & Sons; 2003.
24. Penner, R. A practical guide to patch clamping. In: Sakmann, B.; Neher, E., editors. *Single-Channel Recording*. Springer; 2009. p. 3-30.
25. Hamill OP, Marty A, Neher E, Sakmann B, Sigworth FJ. Improved patch-clamp techniques for high-resolution current recording from cells and cell-free membrane patches. *Pflugers Arch.* 1981; 391:85–100. [PubMed: 6270629]
26. Brown, J.; Hainsworth, A.; Stefani, A.; Randall, A. Whole-cell patch-clamp recording of voltage-sensitive Ca²⁺ channel currents in single cells: heterologous expression systems and neurones. In: Lambert, DG.; Rainbow, RD., editors. *Calcium Signaling Protocols*. Humana Press; 2013. p. 123-148.

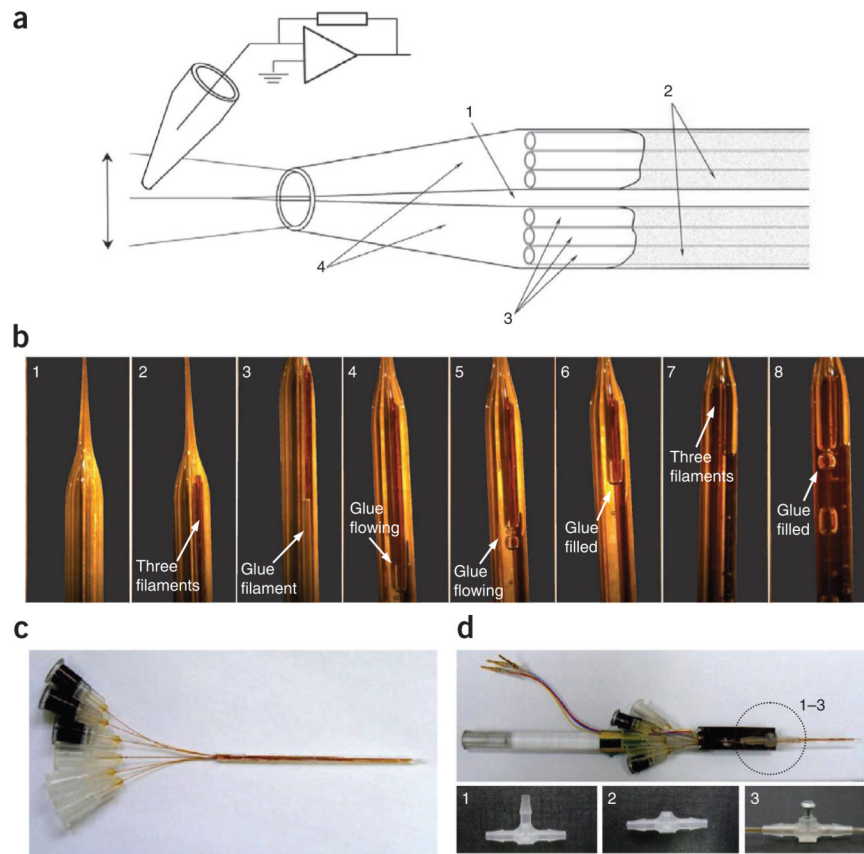


Figure 1.

Preparation of the rapid solution application pipette for RASE. **(a)** Schematic of the solution application θ -glass pipette prepared for RASE (not to scale; the outer pipette diameter ~ 1.5 mm, the open tip diameter ~ 200 μm). 1: θ -glass septum, 2: section of pipette barrels filled with glue, 3: solution supply microfilaments, 4: dead volume near the pipette tip. **(b)** Pipette preparation steps. 1: pipette placed under the microscope, 2: three supply microfilaments inserted into the right channel, 3: an additional microfilament connected to the syringe with glue introduced (arrow), 4–6: stages depicting the right channel being filled with glue, 7: three supply microfilaments inserted into the left channel, 8: both channels are partially filled with glue. **(c)** Pipette with the solution supply microfilaments fixed inside; three filaments and three connectors are marked black and white (unmarked) to distinguish between the two channels. **(d)** Solution application pipette mounted on a piezo-actuator, which is connected to the rod-shaped microelectrode holder. Insets 1–3 (also the dotted circle in the top image): the plastic pipette holder made of a three-way tube connector, with one branch cut off to provide a channel for the tightening screw, as shown (a small piece of silicone inserted in the cutoff channel can help to dampen vibration).

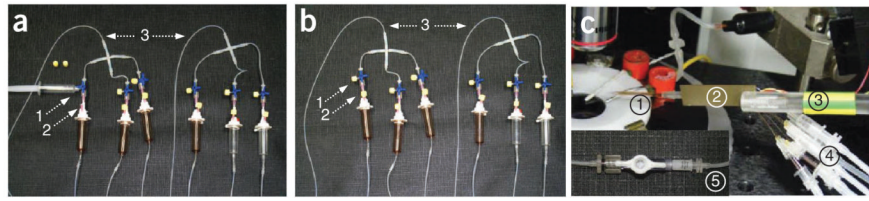


Figure 2.

The arrangement of multiple solution supply and exchange. **(a,b)** Two sets of three liquid containers (plastic cylinders) connected to the pressure supply at one end (3) and to the two θ -glass pipette channels at the other end (shown below in **c**). A connector inlet (1) is connected to the solution-supplying syringe in **a** and closed in **b**. An air outlet (a thick syringe needle embedded into the container plastic; (2)) is open during solution supply in **a** and closed in **b**. Gas pressure lines (3) connect the two container groups to the pneumatic ejector or micropump outlets (not shown). **(c)** A rapid solution application assembly mounted near the recording chamber under a microscope objective including the θ -glass pipette (1), the piezo-actuator (2) and an electrode holder (3), which is set in a position above the recording chamber; six solution supply filaments are connected to the solution supply lines (4) coming from the six corresponding containers (shown in **a,b**). Inset: (5) a 2- μm microfilter inserted into the solution supply line to buffer pressure jumps in the system while providing additional solution filtration.

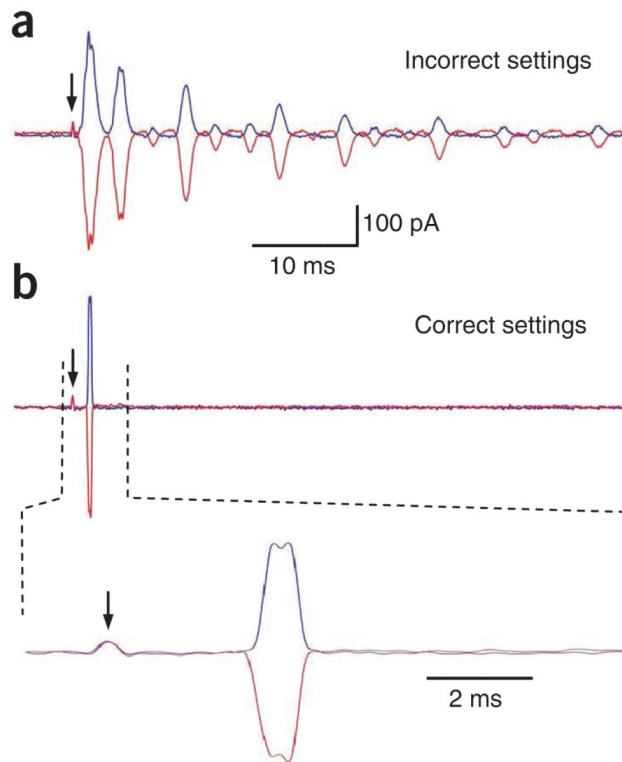


Figure 3. Calibration and adjustment of rapid solution application. **(a)** Red and blue traces illustrate responses to a rapid switch between the distilled water and the ACSF streams in θ -glass pipette channels, before and after full solution replacement (swap over) between the two channels (Supplementary Video 1). The panel shows a characteristic response with suboptimal settings (pipette positioning, ejector pressure, piezo-actuator switch amplitude), leading to characteristic concomitant relaxation waves in the system. For presentation purposes, the currents represented by the red and blue traces were zeroed individually (applies to **a,b**). **(b)** Rapid response under optimized (correct) settings, ensuring a sub-millisecond application time constant (normally 150–200 μ s). With the correct positioning of the recording pipette, a time lag between the piezo-switch artifact (arrow) and the response onset is clearly seen. *Note:* no deflection is seen when both pipette barrels contain the same solution.

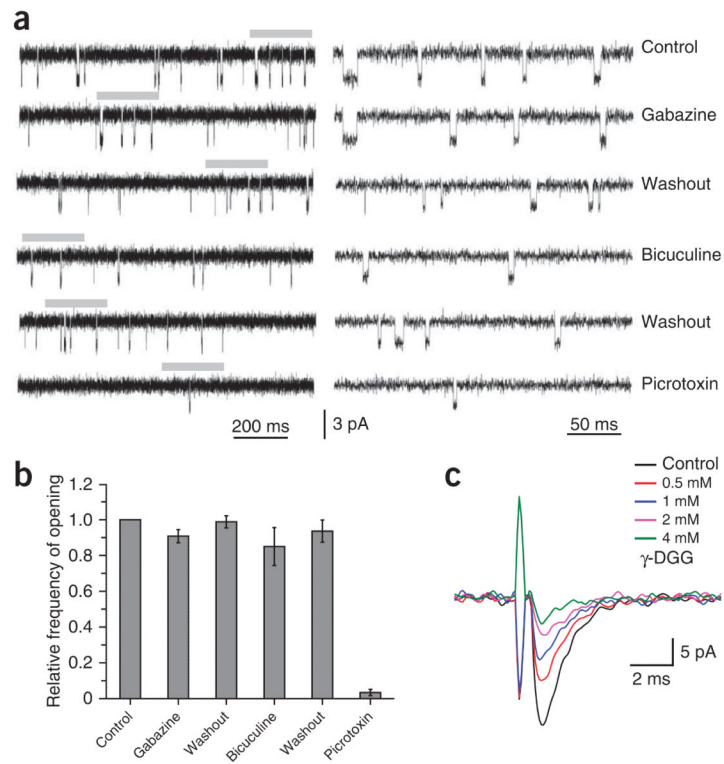


Figure 4.

Examples of protocol implementation in single-channel recordings and in dose-response rapid receptor probing. **(a)** Pharmacological characterization of spontaneously opening individual GABA_A receptors (single channels) in nucleated patches pulled from the dentate gyrus granule cells (acute hippocampal slice). Successive experimental phases are shown, as indicated: control, 25 μ M gabazine, washout, 20 μ M bicuculline, washout, 20 μ M picrotoxin; traces on the right are expanded fragments indicated by gray segments on the left. Solutions in a barrel containing GABA_A receptor antagonists were replaced while patch was exposed to ACSF from another barrel (washout intervals \sim 15 s). **(b)** Statistical summary of experiments shown in **a** (mean \pm s.e.m.; $n = 5$; *** $P < 0.001$); see ref. 21 for further details and explanations. Panels **a** and **b** are modified from ref. 21 with permission. **(c)** Characteristic AMPAR currents in one outside-out patch of a CA1 pyramidal cell evoked by a 1-ms pulse of 1 mM glutamate and the low-affinity antagonist γ -DGG added at four different concentrations in successive trials, as indicated. Four filaments per θ -glass pipette barrel were used in this experiment (each containing ACSF only, ACSF + 1 mM glutamate and ACSF + 1 mM glutamate + one concentration of γ -DGG), and the direction of the rapid solution switch was changed accordingly (reflected in the mirrored piezo-switch deflections) in order to optimize the use of solution supply channels; see ref. 18 for further details and explanations of the corresponding experimental paradigm. To avoid any residual receptor desensitization, intertrial intervals in these and similar experiments were 10–15 s.

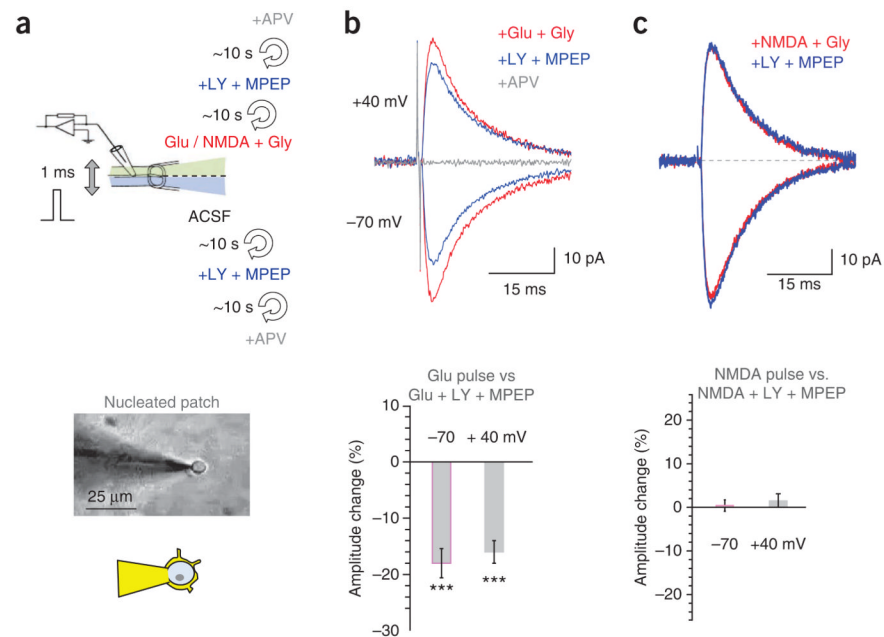


Figure 5.

Examples of protocol implementations in testing mGluR-NMDAR interaction on the millisecond time scale. **(a)** Top: schematic depicting how the θ -glass channel solutions are replaced (within ~ 10 s) during the experiment in which the effect of blocking group I mGluR on NMDAR activation is tested (AMPA and GABA_A receptors are blocked by antagonists present in both pipette channels throughout; see ref. 20 for further protocol detail). The solution replacement order is as shown, from the pipette outward. Bottom: nucleated-patch experiment in acute slices, a DIC image (recording pipette held 15–20- μ m above the slice surface) and a schematic of patch configuration (see Supplementary Video 3 for real-time illustration). **(b)** Traces: NMDAR currents evoked in nucleated patches of CGCs by 1-ms pulses of 1 mM glutamate are inhibited by mGluR1s blockade (LY + MPEP) at both negative and positive holding voltage, characteristic one-patch example; specific NMDAR antagonist APV completely blocks the response. Graph: statistical summary (mean \pm s.e.m., $n = 5$; $***P < 0.005$). **(c)** Traces: similar experiment to one shown in **b**, but with 200 μ M NMDA (which does not activate mGluRs) applied in place of glutamate; no detectable effect of mGluR1 blockade on the NMDA-induced NMDAR response is seen. Graph: statistical summary of the experiment, notation as in **b**. Figure panels are modified from ref. 20 with permission; see the original report for further details and explanations of experimental paradigms.